Original Article

Clinical features and mutation analysis of class 1/2/3 *BRAF* mutation colorectal cancer

Yingying Huang[1], Wenzhuo Jia[2], Gang Zhao[2], Yunbo Zhao[1], Shuai Zhang[1], Zhongkang Li[3], Guoju Wu[1,2]

[1]Department of Oncology, Beijing Hospital, National Center of Gerontology, Beijing, China; [2]Department of Gastrointestinal Surgery, Beijing Hospital, National Center of Gerontology, Beijing, China; [3]Geneplus Beijing, Beijing, China

Contributions: (I) Conception and design: G Wu, Y Huang; (II) Administrative support: G Zhao, W Jia; (III) Provision of study materials or patients: Y Zhao; (IV) Collection and assembly of data: Z Li; (V) Data analysis and interpretation: Z Li, S Zhang; (VI) Manuscript writing: All authors; (VII) Final approval of manuscript: All authors.

Correspondence to: Guoju Wu, MD. Department of Gastrointestinal Surgery, Beijing Hospital, National Center of Gerontology, No. 1 Dahua Road, Dongdan, Dongcheng District, Beijing 100730, China; Department of Oncology, Beijing Hospital, National Center of Gerontology, Beijing, China. Email: 13501359939@163.com.

Background: *BRAF* (B-Raf proto-oncogene, serine/threonine kinase)-mutated colorectal cancer (CRC) still has poor prognostic. The efficacy of *BRAF* inhibitor is unpredictable just that intrinsic genetic complexity, immune microenvironment and partially unknown reason. Understanding the co-mutation mechanism can help improve treatment and follow-up strategies.

Methods: We retrospectively analyzed 35 (*BRAF*-mutated/*BRAF* wild-type) Chinese CRC and 125 Western CRC who underwent next-generation sequencing (NGS). Co-occurrence mutation analysis, Gene Ontology (GO) and Kyoto Encyclopedia of Genes and Genomes (KEGG) pathway enrichment analysis was enabled in this study.

Results: Thirty-five (10.32%) patients were *BRAF*-mutated, with 17 patients were *BRAF* V600E in Beijing Hospital. Patients with *BRAF* mutation had significant association with high tumor mutational burden (TMB-H) (P=0.0004) and high microsatellite instability (MSI-H) (P=0.0003) than those with *BRAF* wild-type. In 125 *BRAF*-mutated Western CRC patients, the frequency of age at diagnosis, gender, sample type, Tumor-Node-Metastasis (TNM), MSI, TMB, and *BRAF* mutation type was consistent with Chinese data. However, the primary tumor location showed significant statistical differences (P<0.0001). Class 1 were more likely to occur in elder and female. Western cohort was consistent with above in Chinese cohort. Other clinicopathological features were not significantly associated with mutation type. However, Western cohort showed class 1 exhibited primary sample type predominance in both class 1 *vs.* others (P<0.05) and class 1 *vs.* class 3 (P<0.05). Meanwhile, the data showed TMB-H (57.69% *vs.* 11.76%, P<0.001) and MSI-H (28.21% *vs.* 0%, P<0.05) of the class 1 *BRAF* mutation proportion were significantly higher, compared with class 3 *BRAF* mutation. In concurrent oncogenic mutations, compared with non-class 1 *BRAF* mutation, class 1 are more likely to co-occur with passenger mutation. Data from Western populations showed similar results. We also found that the class 1 mutation was mutually exclusive with co-*KRAS* (Kirsten rat sarcoma viral oncogene homologue) mutation in CRC, and co-*APC* (APC regulator of WNT signaling pathway) mutation appeared more frequently in non-class 1 *BRAF* mutation. KEGG pathway showed that fewer proto-cancer signaling pathways were enriched in the class 1, which further confirmed that this type had stronger tumorigenicity. GO enrichment also proved that class 1 had stronger tumorigenicity. Finally, prognostic analysis showed median overall survival (mOS) of 19.43 months in class 1 *vs.* 47.57 months in non-class 1 (P=0.0002). Further study showed that the mOS of class 1, class 2, class 3 and class NA (unknown) was 19.43, 28.50, 47.57 months and not reached (P=0.0001), respectively.

Conclusions: This study showed class 1/non-class 1 *BRAF* mutation in CRC had significantly differences in co-mutation features, genomic markers and prognostic. Understanding *BRAF* mutation types and co-mutation mechanism will contribute to accurately grasping treatment and follow-up strategies and promoting

the development of precision therapy for CRC in the future.

Keywords: *BRAF* V600E; colorectal cancer (CRC); co-occurrence mutation analysis; precision therapy

Submitted Oct 08, 2023. Accepted for publication Jan 06, 2024. Published online Feb 05, 2024.
doi: 10.21037/cco-23-117
View this article at: https://dx.doi.org/10.21037/cco-23-117

Introduction

Colorectal cancer (CRC) is the third most commonly diagnosed cancer and the second leading cause for cancer-related deaths worldwide (1,2). In China, CRC ranks fifth among the most frequent malignancies in both incidence and mortality, accounting for more than two-thirds of all cancer cases (3). The efficacy of targeted therapies in CRC patients is largely unpredictable due to intrinsic genetic complexity, immune microenvironment, and partially unknown reason, although significant progress has been made in the development of mutation-driven targeted therapies in CRC patients (4). Therefore, it is urgent to understand the deep molecular mechanisms for CRC patients and improve our understanding of cancer co-mutation feature and overall survival (OS).

BRAF (B-Raf proto-oncogene, serine/threonine kinase) as one of the major oncogenic drivers, occurring in 8–12% CRC patients worldwide and was recently reported to be as high as 20.9% in CRC patients at Beijing Hospital (5,6). More than 70% *BRAF* mutation occur in the kinase domain, including the most commonly observed V600E mutation in CRC (7). A study has elucidated significantly mutually exclusive between *BRAF* and *KRAS* (Kirsten rat sarcoma viral oncogene homologue) mutations (8). *BRAF* inhibitor (*BRAF*i) monotherapy or in combination with an *EGFR* (epidermal growth factor receptor)/*MEK* (mitogen-activated protein kinase kinase 1) inhibitor (*EGFR*i/*MEK*i) have notably improved survival in *BRAF*-mutated solid tumor (9-11). However, *BRAF*-mutated metastatic colorectal cancer (mCRC) has shown a marked lack of sensitivity to *BRAF* or *MEK*i monotherapy in early clinical trials (12). Combined therapy of *BRAF*i and *MEK*i/*EGFR*i can lead to improved clinical outcomes from SWOG S1406 and BEACON CRC study (13,14). A key mechanism is inhibition of *BRAF* leading to increased signaling through the *EGFR* based on negative feedback regulation of signaling pathways in CRC. Therefore, the combination of *BRAF*i and *EGFR*i is more beneficial (15,16). Potential prognostic markers in this field have been discovered in recent years. High *BRAF* allele fraction (AF, ≥2%) showed worse progression-free survival (PFS)/OS than low-*BRAF* AF patients (<2%), suggesting that AF is an independent prognostic factor (17). *RNF43* (ring finger protein 43) mutation could predict response to anti-*BRAF*/*EGFR* combinatory therapies in *BRAF* V600E mCRC (18). Whole transcriptome sequencing (WTS) suggests that a subset of patients with specific molecular features may derive greater clinical benefit from triplet than doublet therapy (19). This biomarker can help tailor patients' treatments. Whereas *BRAF*-mutated melanoma has better efficiency to monotherapy (11). Most of these studies

Highlight box

Key findings

- Patients with *BRAF* (B-Raf proto-oncogene, serine/threonine kinase) mutation had significant association with high tumor mutational burden (TMB-H) and high microsatellite instability (MSI-H), especially in class 1 *BRAF* mutation.
- Class 1 are more likely to co-occur with passenger mutation.
- Class 1 was mutually exclusive with co-*KRAS* mutation and co-*APC* mutation appeared more frequently in non-class 1.
- Median overall survival of class 1/2/3/not available (NA) (unknown) was 19.43/28.50/47.57 months/not reached (P=0.0001), respectively.

What is known and what is new?

- BRAF inhibitor (*BRAF*i) or *BRAF*i + *EGFR* inhibitor/*MEK* inhibitor have notably improved survival in *BRAF*-mutated solid tumors, however, the sensitivity in colorectal cancer (CRC) is to lower. No article reported *BRAF*-mutated concomitant mutation in CRC.
- We analyze class 1/2/3/NA *BRAF* mutation prevalence base on classification system, investigate co-mutation and pathway enrichment in Chinese and Western cohort, and compared the mutation characteristics in two cohort.

What is the implication, and what should change now?

- Class 1 may benefit from *BRAF*i + immunotherapy due to TMB-H and MSI. Understanding *BRAF* mutation types and co-mutation mechanism will promote the development of precision therapy for CRC in the future.

focused on the 600th codon mutation of *BRAF*, and studies have shown that there are significant differences in PFS and OS in patients with different tumor types receiving *BRAF*i therapy. There are also more studies on the combination of *BRAF*i and immunotherapy or chemotherapy. Which one is the best? *BRAF* non-V600E mutation were less discussed and to the best of our knowledge, there are currently no articles reporting *BRAF*-mutated concomitant mutation analysis.

In 2017, a deeper classification system of *BRAF* mutation derived from pre-clinical models functional studies based on kinase activity, *RAS* dependency, dimer dependency and sensitivity to vemurafenib. According to classification system, *RAS*-independent kinase-activating V600 monomers are categorized as class 1, including p.V600E/K/D/R/M; *RAS*-independent kinase-activating dimers that are resistant to vemurafenib are categorized as class 2, including p. K601E/N/T, p. L597Q/V, p. G469A/V/R, p.G464V/E and fusions; and *RAS*-dependent kinase-inactivating heterodimers are categorized as class 3, which consists mainly of p. G466V/E/A, p. D594N/G/A/H and p. G596D/R (20,21). A more in-depth analysis of clinicopathological, prognostic, and co-mutational features based on the *BRAF* mutation classification system is still needed.

In the present study, we retrospectively analyzed the high-throughput sequencing (HTS) data of 339 Chinese CRC from Beijing Hospital to survey the prevalence of class 1/2/3/not available (NA) (unknown) *BRAF* mutations base on classification system, investigated mutation incidence and pathway enrichment in class 1/2/3 *BRAF*-mutated patients, and compared the mutation characteristics of Chinese and Western populations. We aim to find out, through this study, the differences between Chinese and Western *BRAF*-mutated CRC patients, and compare the co-mutation with different *BRAF* mutation types, to make an optimal precision regimen. We present this article in accordance with the STROBE reporting checklist (available at https://cco.amegroups.com/article/view/10.21037/cco-23-117/rc).

Methods

Patients and data collection

Archival samples obtained from 339 CRC patients who underwent targeted capture next-generation sequencing (NGS) between September 2016 to June 2022 at Beijing Hospital (Beijing, China) were included in this case-control study. Tissue samples and peripheral blood samples were collected for genomic sequencing tests and as germline controls, respectively. The clinicopathological features were collected from patient medical records, which are summarized in *Table 1*. The study was conducted in accordance with the Declaration of Helsinki (as revised in 2013). The study was approved by the Ethics Committee of Beijing Hospital (No. 2023BJYYEC-103-01) and informed consent was taken from all the patients.

We also conducted a cohort comparison of Chinese and Western populations from Memorial Sloan-Kettering Cancer Center (MSKCC) (22,23). On the one hand, MSKCC datasets focusing on metastasis CRC were selected to match the Chinese cohort TNM (Tumor-Node-Metastasis) staging, and on the other hand, batch datasets could eliminate the bias of artificial selection of data, thus making the analysis results more credible. The somatic mutation data and the clinicopathological information of patients with 125 CRC data were downloaded from the cBioPortal platform (http://www.cbioportal.org).

DNA isolation and targeted capture sequencing

Genome DNA (gDNA) was extracted from formalin-fixed, paraffin-embedded (FFPE) tissue samples and peripheral blood lymphocytes (PBL) using TIANamp Blood DNA Kits and TIANamp Genomic DNA Kits (Tiangen Biotech, China), respectively. DNA quality was controlled using Qubit®2.0 fluorimeter (Life Technologies, USA) and 2100 Bioanalyzer (Agilent, USA). Target DNA capture was performed using the 1,021 panel (Geneplus, China; table available at https://cdn.amegroups.cn/static/public/cco-23-117-1.xlsx), a custom-designed biotinylated oligonucleotide probes (Roche NimbleGen, Madison, WI, USA) covering ~1.4 Mbp coding region of genomic sequence of 1,021 cancer-related genes. Libraries were constructed using the Hieff NGS Ultima DNA Library Prep Kit (Yeasen Biotechnology, Shanghai, China). High throughput sequencing was performed on an Illumina HiSeq 2000/2500 platform (Illumina, San Diego, CA, USA) to generate 101 bp paired-end reads.

NGS analysis

Quality metrics were performed on raw data using NCfilter and aligned to the human genome build GRCh37 using Burrows-Wheeler Aligner (BWA) (24). Picard (http://broadinstitute.github.io/picard/) were used to mark PCR

Table 1 Clinical characteristics and molecular characteristics of colorectal cancer patients in the Chinese cohort

Characteristics	Total (n=339)	*BRAF* mutation (n=35)	*BRAF* wild-type (n=304)	P value
Age at diagnosis (years)				NA
Median	63	62	63	
Range	25–93	28–87	25–93	
Gender, n (%)				0.6261
Male	189 (55.75)	19 (54.29)	170 (55.92)	
Female	143 (42.18)	16 (45.71)	127 (41.78)	
NA	7 (2.06)	0	7 (2.30)	
Sample type, n (%)				0.4463
Primary	230 (67.85)	26 (74.29)	204 (67.11)	
Metastasis	66 (19.47)	4 (11.43)	62 (20.39)	
NA	43 (12.68)	5 (14.29)	38 (12.50)	
Primary tumor location, n (%)				0.842
Left	186 (54.87)	18 (51.43)	168 (55.26)	
Right	42 (12.39)	4 (11.43)	38 (12.50)	
NA	111 (32.74)	13 (37.14)	98 (32.24)	
TNM, n (%)				0.5788
I	3 (0.88)	1 (2.86)	2 (0.66)	
II	9 (2.65)	0	9 (2.96)	
III	25 (7.37)	3 (8.57)	22 (7.24)	
IV	229 (67.55)	24 (68.57)	205 (67.43)	
NA	73 (21.53)	7 (20.00)	66 (21.71)	
TMB, n (%)				0.0004*
TMB-H	29 (8.55)	9 (25.71)	20 (6.58)	
TMB-L	296 (87.32)	26 (74.29)	270 (88.82)	
NA	14 (4.13)	0	14 (4.61)	
MSI, n (%)				0.0003*
MSS	302 (89.09)	28 (80.00)	280 (92.11)	
MSI-H	19 (5.60)	7 (20.00)	12 (3.95)	
NA	18 (5.31)	0	12 (3.95)	
BRAF mutation type, n (%)				NA
Class 1	–	17 (48.57)	–	
Class 2	–	4 (11.43)	–	
Class 3	–	9 (25.71)	–	
Class NA (unknown)	–	5 (14.29)	–	

*, statistical significance. NA, not available; TNM, Tumor-Node-Metastasis; TMB, tumor mutational burden; TMB-H, high TMB; TMB-L, low TMB; MSI, microsatellite instability; MSS, microsatellite stability; MSI-H, high MSI.

duplicates. Somatic mutation single nucleotide variant (SNV) and Indels were performed using MuTect2 (25) and GATK (26), respectively. Somatic structural variant (SV) mutation was called using NCsv software (Geneplus, China). PBL NGS results were used to filter germline mutation. All candidate somatic mutations were manually reviewed using Integrated Genomics Viewer (IGV) (27) to filter out false positives. The mutated protein coding position and filtered intronic and silent changes were annotated by ANNOVAR software (28). The 1,021-panel has corrected coverage data for GC content and sequencing bias resulting from probe design, which can eliminate bias in mutation analysis.

Tumor mutational burden (TMB) and microsatellite instability (MSI) status analysis

The TMB in the Chinese cohort was defined as the number of non-silent somatic mutations (non-synonymous single nucleotide variation "SNV", indel, and splice ±2) per mega-base (1 Mb) of coding genomic regions sequenced (1.03 Mb for this 1,021 panel) (29). The TMB in Western cohort from MSKCC adds an additional frameshift variant type. In the present study, the upper quartile of TMB was deemed as high TMB (TMB-H) (22,23). The threshold values of the Chinese cohort and Western cohort were 9 and 11.74 mutations/Mb, respectively. The MSI status of NGS data in Chinese cohort were inferred using MSIsensor (v0.2), which reported the percentage of unstable somatic microsatellites through Chi-square test on predefined microsatellite regions covered by 1,021 panel. Default parameters were used (30). The Western cohort of MSI status was also calculated by MSI sensor (22,31) and the data were download as described above.

Statistical analysis

Analysis of differences among two groups were calculated and presented using either Fisher's exact test or paired, two-tailed Student's *t*-test. Univariate logistic regression was used to analyze the correlation between *BRAF* mutation status, others mutation and clinical features. Survival curves were estimated by Kaplan-Meier method and differences among designed groups were tested by log-rank test. P values <0.05 was denoted as statistically significant. All the data were analyzed using R statistics package (R version 4.2.1, Austria) or GraphPad Prism version 8 (GraphPad Software, CA, USA).

Mutation analysis and functional enrichment

Co-occurrence mutation analysis was performed using R statistics package, which was used to explore consistency and differences in class 1/2/3/NA *BRAF* mutation cohort. Also, in this present study, we explored the main biological functions of the identified statistically significant gene via the Gene Ontology (GO) and Kyoto Encyclopedia of Genes and Genomes (KEGG) pathway enrichment analysis. David 6.8 (https://david.ncifcrf.gov/) was used to carried out the GO and KEGG pathway enrichment analysis.

Results

Patient characteristics

Overall, 339 Chinese CRC patients were retrospectively reviewed in Beijing Hospital. Thirty-five (10.32%) patients carried *BRAF* mutation, with a total of 17 patient tissues (48.57%) were *BRAF* V600E. All patients were updated according to the 8th edition of the TNM staging criteria. Most patients were diagnosed at stage IV disease (229/339, 67.55%). Besides, patients with primary cancer were the most type (230/339, 67.85%). Regarding primary tumor location, 186 (54.87%), 42 (12.39%), and 111 (32.74%) patients were diagnosed with left-sided, right-sided and NA primary tumor location in total patients. There were 4 (11.43%) right-sided (cecum to transverse colon) and 18 (51.43%) left-sided (splenic flexure to sigmoid colon) in *BRAF*-mutated population. This was inconsistent with previous literatures (7), which may be related to the sample size, but there was no significant statistical difference (P=0.842). According to our analysis, patients with *BRAF* mutation had significant association with TMB-H and high MSI (MSI-H) than those with *BRAF* wild-type (P=0.0004 for TMB, P=0.0003 for MSI). The clinical and pathological features are showed in *Table 1*.

In this study, 125 Western CRC patients, including 67 men (53.60%) and 58 women (46.40%), were brought into study from the cBioPortal database. Most patients were diagnosed at stage IV disease (72/125, 57.60%). The frequencies of age at diagnosis, gender, sample type, stage (TNM), MSI, TMB, and *BRAF* mutation type were consistent with the Chinese population. However, the primary tumor location showed significant statistical differences (P<0.0001). Fifty-two (41.60%) and 72 (57.60%) were diagnosed with left-sided and right-sided primary tumor location, respectively (table available at https://cdn.amegroups.cn/static/public/cco-23-117-2.xlsx).

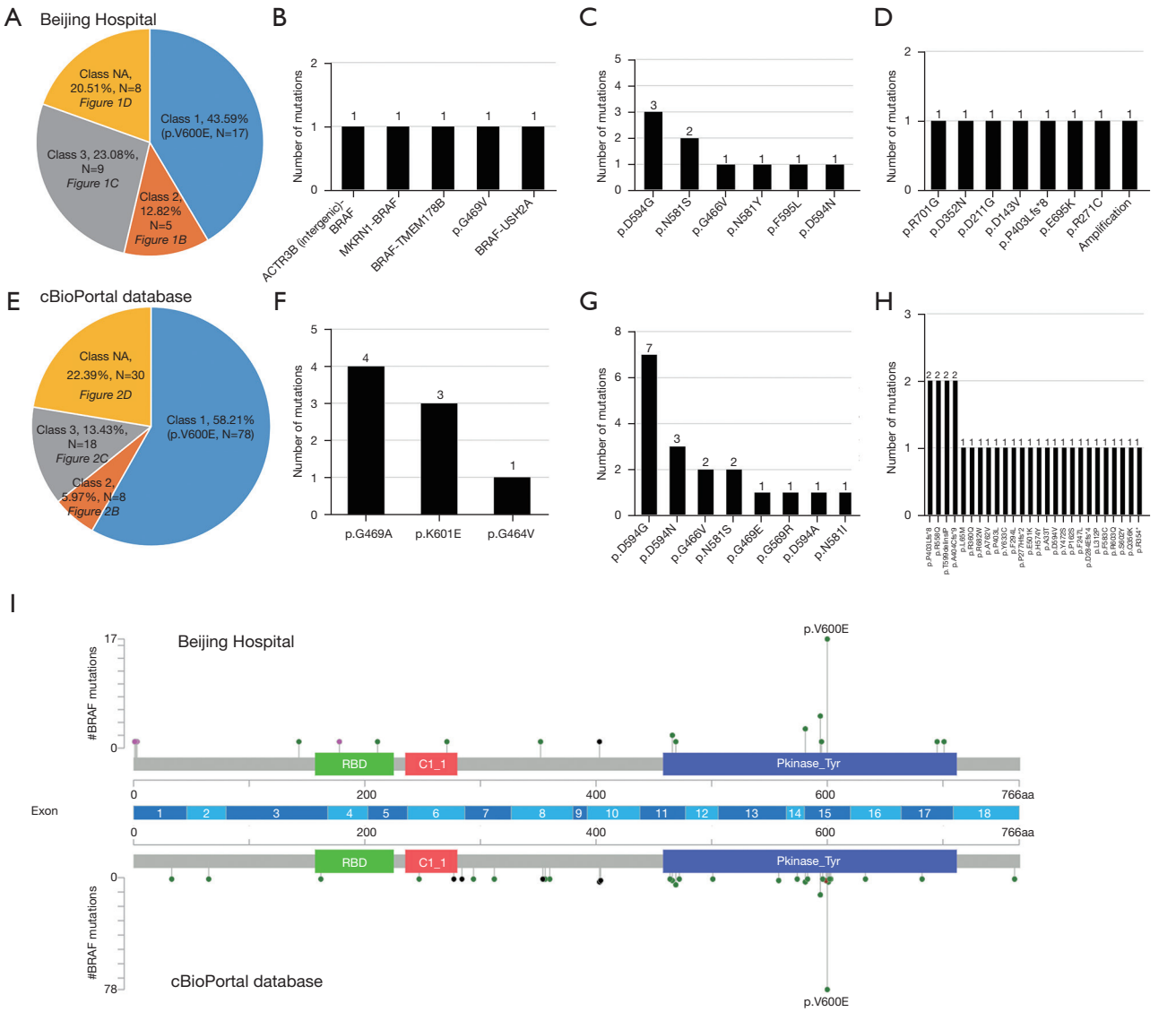

Figure 1 A panoramic analysis of the incidence, distribution and classification of *BRAF* mutations. Distribution of *BRAF*-mutated patients categorized according to classification system in the Chinese cohort (A) and the Western cohort (E). The detection patient number of the mutations in class 2 (B, Chinese cohort; F, Western cohort), class 3 (C,G) and class NA (D,H). X-axis denotes the *BRAF* mutations. Y-axis denotes the mutation detection number. (I) Lollipop plots (maps mutations on a linear protein and its domains) between the Chinese cohort and Western cohort. NA, not available.

Prevalence of BRAF mutation and co-mutation features

Of the analyzed patients, a total of 39 and 134 *BRAF* mutation were detected in the Chinese cohort and the Western cohort, respectively. Class 1 *BRAF* mutation, all of them was p.V600E, were mostly dominant mutation (*Figure 1*). We first analyzed the types and distribution of *BRAF* mutations, as well as the differences in the incidence of *BRAF* mutations in the Chinese and Western cohort and pathway enrichment analysis was also performed. Then, we analyzed the mutation spectrum and con-mutation differences between class 1 *BRAF* mutation and other types of *BRAF* mutations (based on classification system) (20), and the KEGG pathway enrichment was also performed. We also compared *BRAF* mutation and BRAF wild-type populations as described in the analysis above.

Table 2 Clinical characteristics and molecular characteristics analysis between class 1 *BRAF* mutation and non-class 1 *BRAF* mutations in the Chinese colorectal cancer cohort

Characteristics	Class 1 (n=17)	Non-class 1 (n=18)	P value
Age, n (%)			0.18
Young	1 (5.88)	5 (27.78)	
Intermediate	8 (47.06)	8 (44.44)	
Elder	7 (41.18)	4 (22.22)	
NA	1 (5.88)	1 (5.56)	
Gender, n (%)			0.18
Male	7 (41.18)	12 (66.67)	
Female	10 (58.82)	6 (33.33)	
Sample type, n (%)			>0.99
Primary	11 (64.71)	15 (83.33)	
Metastasis	2 (11.76)	2 (11.11)	
NA	4 (23.53)	1 (5.56)	
Primary tumor location, n (%)			0.112
Left	9 (52.94)	9 (50.00)	
Right	4 (23.53)	0	
NA	4 (23.53)	9 (50.00)	
MSI, n (%)			>0.99
MSI-H	3 (17.65)	4 (22.22)	
MSS	14 (82.35)	14 (77.78)	
TMB, n (%)			0.443
TMB-H	3 (17.65)	6 (33.33)	
TMB-L	14 (82.35)	12 (66.67)	

NA, not available; MSI, microsatellite instability; MSI-H, high MSI; MSS, microsatellite stability; TMB, tumor mutational burden; TMB-H, high TMB; TMB-L, low TMB.

In the Chinese cohort, 35 patients carried 39 *BRAF* mutation, with 43.59% (17/39), 12.82% (5/39), 23.08% (9/39) and 20.51% (8/39) patients had class 1, 2, 3 and NA *BRAF* mutations, respectively (*Figure 1A*). The specific distributions of patients with class 2, 3 and NA were depicted in *Figure 1B-1D*, respectively. The class 2 *BRAF* mutation subgroup consisted of four fusion mutation types [*ACTR3B* (intergenic)-*BRAF*, *MKRN1-BRAF*, *BRAF-TMEM178B*, *BRAF-USH2A*) and one missense (p.G469V) (table available at https://cdn.amegroups.cn/static/public/cco-23-117-3.xlsx). Of the patients with class 3 *BRAF* mutation, six missenses were found, including p.D594G [3], p.N581S [2], p.G466V [1], p.N581Y [1], p.F595L [1], p.D594N [1]. Furthermore, 11 *BRAF* mutations were classified as undefined. Among them, six were missense types (p.R701G, p.D352N, p.D211G, p.D143V, p.E695K, p.R271C), one was frameshift (p.P403Lfs*8) and one was *BRAF* amplification. Meanwhile, four patients (11.43%, 4/35) had compound *BRAF* mutation. All of them belong to non-class 1 *BRAF* mutations (table available at https://cdn.amegroups.cn/static/public/cco-23-117-4.xlsx).

In Western cohort, the distribution of patients with class 1, 2, 3 and NA were 58.21% (78/134), 5.97% (8/134), 13.43% (18/134) and 22.39% (30/134), respectively (*Figure 1E*). Only three missenses were found in class 2 *BRAF* mutation, including p.G469A [4], p.K601E [3], p.G464V [1], which may be due to the lack of analysis of SV and copy number variation (CNV) in this study (*Figure 1F*). Among the class 3 *BRAF* mutations (*Figure 1G*), the Western population and the Chinese population showed a high mutation consistency, manifested as a relatively higher mutation frequency of p.D594G and p.N581S. Moreover, 21 missense, one nonsense and eight frameshifts were defined as class NA subgroup, among them manifested the characteristics of wide and irregular distribution (*Figure 1H*, table available at https://cdn.amegroups.cn/static/public/cco-23-117-3.xlsx).

Next, we investigated the correlation between *BRAF* mutation and clinicopathological features. In the Chinese cohort, class 1 *BRAF* mutation was more likely to occur in elder (41.18% *vs.* 22.22%, P=0.18) and female (58.82% *vs.* 33.33%, P=0.18), although no statistical difference was presented. Other clinicopathological features, including sample type, primary tumor location, TMB and MSI were not significantly associated with *BRAF* mutation types (*Table 2*).

We further analyzed the Western cohort and the data were shown in *Table 3*. Consistent with the Chinese data, class 1 *BRAF* mutation was more common in elderly patients (29.49% *vs.* 14.89%), non-class 1 *BRAF* mutations were more likely to occur in younger patients (24.36% *vs.* 42.55%). We compared the distribution of different *BRAF* mutation types between the genders. The results showed that class 1 were more likely to occur in female than non-class 1 mutations (53.85% *vs.* 34.04%, P<0.05). There is no significant difference between class 2 *vs.* class 3, class 1 *vs.* class 2, and class 1 *vs.* class 3 (28.57% *vs.* 41.18%, P=0.67; 53.85% *vs.* 28.57%, P=0.25; 53.85% *vs.* 41.18%, P=0.43). When sample type distribution was analyzed, class 1 exhibited primary predominance in both class 1 *vs.* others

Table 3 Clinical characteristics and molecular characteristics analysis between class 1 *BRAF* mutation and non-class 1 *BRAF* mutations in the Western colorectal cancer cohort

Characteristics	Class 1 (n=78)	Others (n=47)				P value			
		Total (n=47)	Class 2 (n=7)	Class 3 (n=17)	NA (n=23)	Class 1 *vs.* others	Class 2 *vs.* class 3	Class 1 *vs.* class 2	Class 1 *vs.* class 3
Age, n (%)						0.055	0.9378	0.499	0.5087
Young	19 (24.36)	20 (42.55)	3 (42.86)	6 (35.29)	11 (47.83)				
Intermediate	36 (46.15)	20 (42.55)	3 (42.86)	8 (47.06)	9 (39.13)				
Elder	23 (29.49)	7 (14.89)	1 (14.29)	3 (17.65)	3 (13.04)				
Gender, n (%)						0.0417*	0.6687	0.2547	0.4257
Male	36 (46.15)	31 (65.96)	5 (71.43)	10 (58.82)	16 (69.57)				
Female	42 (53.85)	16 (34.04)	2 (28.57)	7 (41.18)	7 (30.43)				
Sample type, n (%)						0.0184*	>0.99	0.1941	0.0237*
Primary	53 (67.95)	22 (46.81)	3 (42.86)	7 (41.18)	12 (52.17)				
Metastasis	21 (26.92)	23 (48.94)	4 (57.14)	10 (58.82)	9 (39.13)				
NA	4 (5.13)	2 (4.26)	0	0	2 (8.70)				
Primary tumor location, n (%)						0.0014*	>0.99	0.0428*	0.0088*
Left	24 (30.77)	28 (59.57)	5 (71.43)	11 (64.71)	12 (52.17)				
Right	54 (69.23)	18 (38.30)	2 (28.57)	5 (29.41)	11 (47.83)				
NA	0	1 (2.13)	0	1 (5.88)	0				
MSI, n (%)						0.0642	0.2105	>0.99	0.008*
MSS	41 (52.56)	31 (65.96)	3 (42.86)	15 (88.24)	13 (56.52)				
MSI-H	22 (28.21)	6 (12.77)	1 (14.29)	0	5 (21.74)				
NA	15 (19.23)	10 (21.28)	3 (42.86)	2 (11.76)	5 (21.74)				
TMB, n (%)						0.139	0.1265	0.6937	0.0009*
TMB-H	45 (57.69)	20 (42.55)	3 (42.86)	2 (11.76)	15 (65.22)				
TMB-L	33 (42.31)	27 (57.45)	4 (57.14)	15 (88.24)	8 (34.78)				

*, statistical significance. NA, not available; MSI, microsatellite instability; MSI-H, high MSI; MSS, microsatellite stability; TMB, tumor mutational burden; TMB-H, high TMB; TMB-L, low TMB.

(67.95% *vs.* 46.81%, P<0.05) and class 1 *vs.* class 3 (67.95% *vs.* 41.18%, P<0.05). To study primary tumor location, we found right-sided CRC was more likely to occur in class 1 (class 1 *vs.* others: 69.23% *vs.* 38.30%, P<0.05; class 1 *vs.* class 2: 69.23% *vs.* 28.57%, P<0.05; class 1 *vs.* class 3: 69.23% *vs.* 29.41%, P<0.05), which was inconsistent with the data analyzed above (*Table 2*). Meanwhile, we examined the relationship between genomic markers—TMB, MSI and *BRAF* mutation types. The data showed that the proportion of TMB-H (57.69% *vs.* 11.76%, P<0.001) and MSI-H (28.21% *vs.* 0%, P<0.05) in *BRAF* class 1 mutations was significantly higher than that in *BRAF* class 3 mutations.

Concurrent oncogenic mutations

We further analyzed the distribution of concurrent oncogenic mutations between the Chinese cohort and Western cohort. A total of 339 Chinese patients were tested by 1,021-gene panel NGS, 125 Western patients were tested by MSK-IMPACT (table available at https://cdn.amegroups.cn/static/public/cco-23-117-5.xlsx).

The rate of concomitant mutation of class 1/2/3/NA

BRAF mutations in patients from the two cohorts are given in *Figure 2*. Collectively, the top 10 concurrent mutation frequencies of class 1 *BRAF* mutation in the Chinese population were in *TP53* (tumor protein p53) (65%), *PTEN* (phosphatase and tensin homolog) (35%), *RNF43* (29%), *MLL2* (24%), *MLL3* (24%), *NOTCH1* (24%), *PIK3CA* (24%), *SMAD4* (24%), *TGFBR2* (24%) and *APC* (APC regulator of WNT signaling pathway) (18%). It was found that *APC* (67%) was the highest mutation frequency in top 10 non-class 1 *BRAF* mutations, followed by *TP53* (67%), *KRAS* (56%), *LRP1B* (44%), *FBXW7* (39%), *AXIN2* (28%), *FGFR1* (fibroblast growth factor receptor 1) (28%), *NOTCH1* (28%), *PIK3CA* (28%) and *PPP2R1A* (28%).

Class 1 *BRAF* mutation has a lower concomitant mutation frequency, and also tends to be accompanied by co-mutation of passenger genes in the Chinese population (*Figure 2A*,*2B*). Identical results were obtained from the Western population (*Figure 2C*,*2D*). In addition, we compared *BRAF* mutation types and wild-type in the Chinese population. The top 10 concomitant mutations of *BRAF* mutation in the Chinese population were in *TP53* (66%), *APC* (43%), *LRP1B* (31%), *KRAS* (29%), *FBXW7* (26%), *NOTCH1* (26%), *PIK3CA* (26%), *FAT2* (20%), *MLL2* (20%), and *MLL3* (20%), while those of *BRAF* wild-type (table available at https://cdn.amegroups.cn/static/public/cco-23-117-6.xlsx) were in *TP53* (77%), *APC* (67%), *KRAS* (49%), *PIK3CA* (18%), *SMAD4* (18%), *TCF7L2* (18%), *FBXW7* (17%), *MYC* (17%), *LRP1B* (16%), and *PTEN* (11%). We can find that *BRAF* wild-type is associated with higher frequencies of concomitant mutation, mainly manifested in the tumor suppressor genes *TP53* and *APC*, as well as tumor driver gene *KRAS* in the Chinese cohort. The above two findings did not show significant differences (Figure S1). The results suggest that class 1/non-class 1 *BRAF* mutations and *BRAF* wild-type have significant differences in carcinogenicity.

Meanwhile, we compared the co-occurrence and mutual exclusion of core driver gene mutations in the two cohorts (*Table 4*). *KRAS* was significantly enriched in the non-class 1 *BRAF* mutations, indicating that *KRAS* and class 1 *BRAF* mutation are mutually exclusive in the Chinese cohort (P=0.0003), and Western cohort (P=0.0001). None of the 35 patients with class 1 *BRAF* mutation had co-*KRAS* mutation. However, three patients with class 2, four patients with class 3 and three patients with class NA *BRAF* mutation had concurrent oncogenic *KRAS* mutation (most of the sites were p.A146X, and no p.G12C appeared) (P<0.001) in the Chinese cohort. At the same time, we analyzed the Western cohort data, and found four class 1 *BRAF*-mutated patients co-occurred with *KRAS* (p.G12A, p.G13D, p.I171Nfs*14, p.G12D). The numbers of class 2, class 3 and class NA *BRAF*-mutated patients with co-*KRAS* mutation were 0, 3 and 12, respectively. In addition, we found that there was no class 2 *BRAF* mutations in the Western cohort, which may be related to the absence of fusion mutation in the MSKCC, because there were three class 2 co-mutation patients in the Chinese cohort, all of which were *BRAF* fusion with co-*KRAS* mutation. The result is shown in *Figure 3*. Also, we found that co-*APC* mutation was significantly enriched in the non-class 1 *BRAF* mutations (P=0.0059 in the Chinese cohort, P<0.0001 in the Western cohort). Since the *APC* gene is a typical diagnostic marker for CRC, it has a significantly longer tumor formation period, which suggests that patients with non-class 1 *BRAF* mutations have a longer tumor formation period and relatively lighter carcinogenesis than class 1 patients. Considering the limited race characteristics, differences between the two cohorts may have occurred. Co-*PTEN* mutation and co-*FGFR1* mutation were significantly enriched in the class 1 *BRAF*-mutated and non-class 1 *BRAF*-mutated Chinese population, respectively, while no statistical difference was found in the Western cohort. In contrast, co-*RNF43* mutation and non-*TP53* mutation were significantly enriched in the class 1 *BRAF*-mutated Western population, whereas in the Chinese cohort, no statistical difference was found.

KEGG pathway and GO enrichment

We analyzed the enrichment results of signature mutations of class 1 and non-class 1 populations. We first counted the unique mutations between class 1 *BRAF* mutation and non-class 1 *BRAF* mutations, and then used the Fisher test to count the incidence of genes that coexist in the two groups. Genes with P<0.05 and odds ratio (OR) >1 were incorporated into non-class 1 unique mutation set, while genes with P<0.05 and OR <1 were incorporated into class 1 *BRAF*-mutated unique mutation set.

The KEGG pathway enrichment results showed that class 1 *BRAF* mutation was enriched with fewer proto-cancer signaling pathways, which further proved that class 1 *BRAF* mutation has stronger tumorigenicity. GO enrichment results showed that the most common pathway in class 1 *BRAF* mutation was GO:0000122/0045944 (type II RNA polymerase promoter transcriptional regulator), while the pathway in the non-class 1 *BRAF* mutations

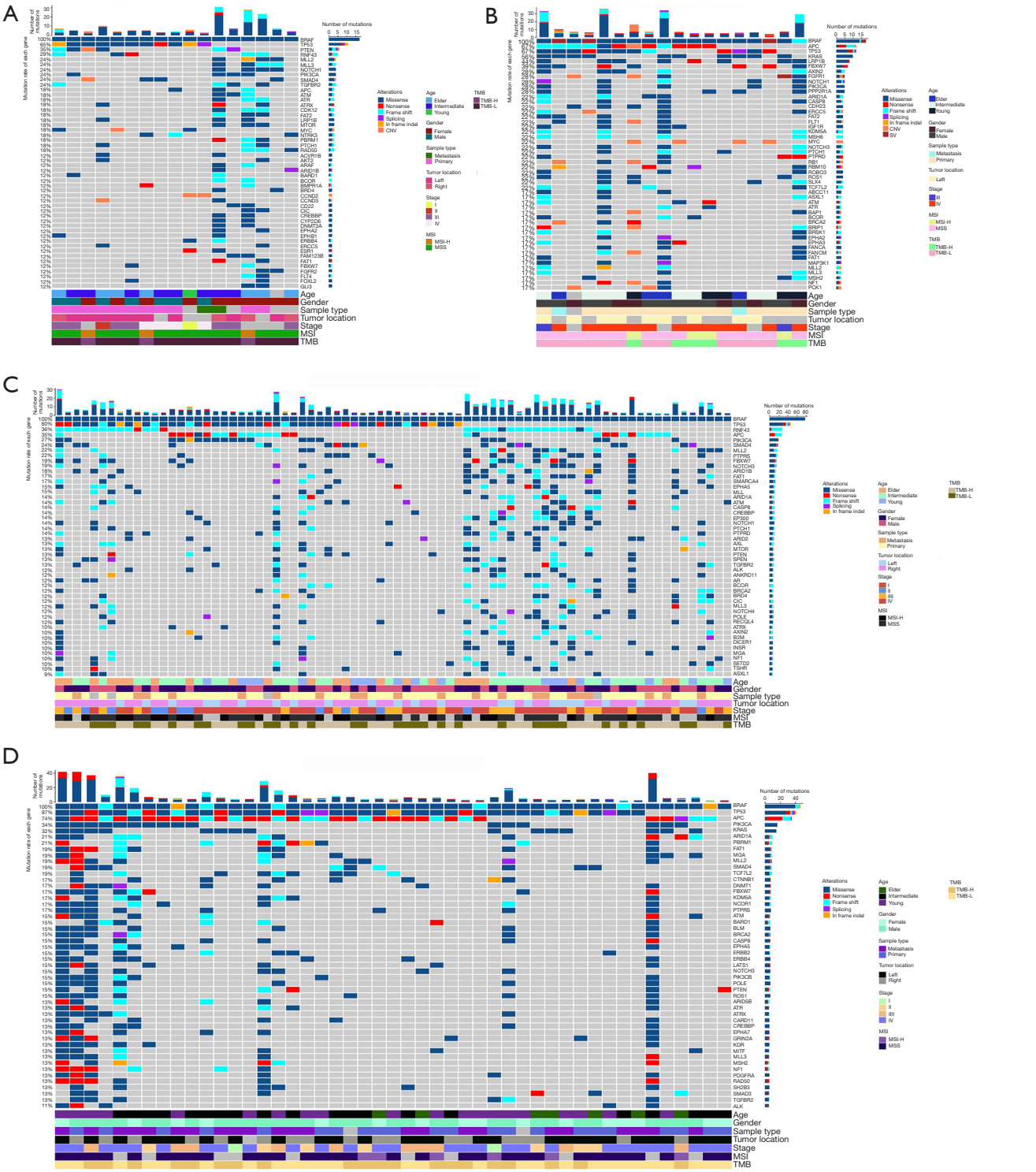

Figure 2 Top 50 mutation spectrum in the Chinese cohort (A, class 1 *BRAF* mutation; B, non-class 1 *BRAF* mutations) and the Western cohort (C, class 1 *BRAF* mutation; D, non-class 1 *BRAF* mutations). Each column represents a patient and each row represents a gene. Table on the left represents the mutation rate of each gene. Top plot represents the overall number of mutations a patient carried. Different colors denote different types of mutations. CNV, copy number variation; MSI-H, high microsatellite instability; MSS, microsatellite stability; TMB, tumor mutational burden; TMB-H, high TMB; TMB-L, low TMB; SV, structural variation.

Table 4 Comparison the co-occurrence and mutual exclusion of core driver gene mutations between the two cohorts of *BRAF* mutation classification

Cohort	Characteristics	Class 1	Non-Class 1	P value	95% CI
Beijing Hospital	Co-*KRAS*mt	0	10	0.0003	0.000 to 0.2417
	Non-*KRAS*mt	17	8		
cBioPortal database	Co-*KRAS*mt	4	15	0.0001	0.03990 to 0.3752
	Non-*KRAS*mt	74	32		
Beijing Hospital	Co-*APC*mt	3	12	0.0059	0.02696 to 0.5510
	Non-*APC*mt	14	6		
cBioPortal database	Co-*APC*mt	27	35	<0.0001	0.08421 to 0.3965
	Non-*APC*mt	51	12		
Beijing Hospital	Co-*PTEN*mt	6	1	0.0408	1.072 to 111.5
	Non-*PTEN*mt	11	17		
cBioPortal database	Co-*PTEN*mt	10	7	0.791	0.3179 to 2.205
	Non-*PTEN*mt	68	40		
Beijing Hospital	Co-*FGFR1*mt	0	5	0.0455	0.000 to 0.4643
	Non-*FGFR1*mt	17	13		
cBioPortal database	Co-*FGFR1*mt	3	2	>0.9999	0.1784 to 5.226
	Non-*FGFR1*mt	75	45		
Beijing Hospital	Co-*FGFR1*mt	5	2	0.2285	0.05445 to 1.971
	Non-*FGFR1*mt	12	16		
cBioPortal database	Co-*FGFR1*mt	28	4	0.0002	2.542 to 26.78
	Non-*FGFR1*mt	50	43		
Beijing Hospital	Co-*TP53*mt	11	12	>0.9999	0.2496 to 3.354
	Non-*TP53*mt	6	6		
cBioPortal database	Co-*TP53*mt	47	41	0.0013	0.08688 to 0.5595
	Non-*TP53*mt	31	6		
Beijing Hospital	Co-*FBXW7*mt	2	7	0.1212	0.03991 to 1.078
	Non-*FBXW7*mt	15	11		
cBioPortal database	Co-*FBXW7*mt	15	8	0.8158	0.4744 to 2.975
	Non-*FBXW7*mt	63	39		
Beijing Hospital	Co-*LRP1B*mt	3	8	0.1464	0.06666 to 1.221
	Non-*LRP1B*mt	14	10		
cBioPortal database	Co-*LRP1B*mt	NA	NA	NA	NA
	Non-*LRP1B*mt	NA	NA		
Beijing Hospital	Co-*AXIN2*mt	1	5	0.1774	0.01311 to 1.217
	Non-*AXIN2*mt	16	13		
cBioPortal database	Co-*AXIN2*mt	8	3	0.5334	0.4699 to 6.072
	Non-*AXIN2*mt	70	44		
Beijing Hospital	Co-*PPP2R1A*mt	1	5	0.1774	0.01311 to 1.217
	Non-*PPP2R1A*mt	16	13		
cBioPortal database	Co-*PPP2R1A*mt	NA	NA	NA	NA
	Non-*PPP2R1A*mt	NA	NA		

Mut, mutation; CI, confidence interval; NA, not available.

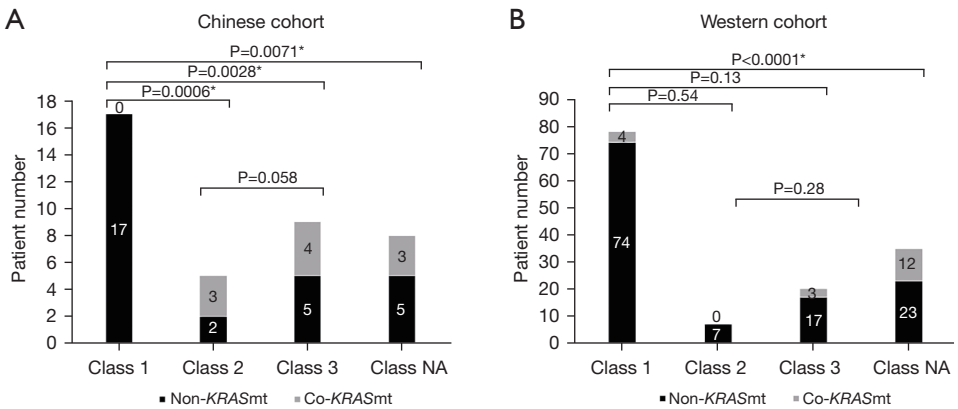

Figure 3 Concurrent *KRAS* mutations in different *BRAF* mutations. Class 1 *BRAF* mutation was mutually exclusive from *KRAS* in the Chinese cohort (A) and the Western cohort (B). *, statistical significance. NA, not available; mt, mutation.

included GO:0008285 (cell proliferation regulation), GO:0010628 (regulation of gene expression), GO:0051726 (regulation of cell cycle), etc., which prove that class 1 *BRAF* mutation has stronger tumorigenicity (*Figure 4*). Meanwhile, we explored the difference in KEGG pathway enrichment between *BRAF* wild type and *BRAF* mutations, and the results showed that compared with *BRAF* wild type, *BRAF* mutations have stronger carcinogenicity, which is consistent with the enrichment pathway analyzed above [GO:0000122/0045944 (type II RNA polymerase promoter transcriptional regulator) pathway] (Figure S2).

Survival outcomes

We also analyzed survival outcomes based on *BRAF* mutation types in 125 patients with evaluable stage I–IV CRC (*Figure 5*). First, we compared the survival outcomes of 78 patients with class 1 *BRAF* mutation and 47 patients with non-class 1 *BRAF* mutations. Kaplan-Meier and log-rank analysis showed that patients with non-class 1 *BRAF* mutations had longer OS (P=0.0002), with median OS of 47.57 *vs.* 19.43 months, respectively. Second, we divided *BRAF* mutations into four categories: class 1 (n=78)/2 (n=7)/3 (n=17)/NA (n=23). Kaplan-Meier and log-rank analysis showed that the median OS of the four types of *BRAF* population was 19.43 *vs.* 28.50 *vs.* 47.57 months *vs.* not reached (P=0.0001).

Discussion

Our study tried to compare the differences in concomitant mutational patterns between the Chinese and Western populations with CRC and their correlation with clinicopathological features. We found that class 1 *BRAF* mutation was more common in elderly and female patients in both Chinese and Western populations, while non-class 1 *BRAF* mutations were more likely to occur in younger patients in the Western population. Additionally, we found that class 1 *BRAF* mutation was more likely to be accompanied by passenger gene mutations, and rich in oncogenic signaling pathways compared to non-class 1 *BRAF* mutations in the Chinese population. This means that *BRAF* V600E could be the main important driver mutation. Furthermore, our results showed that TMB-H and MSI-H were significantly associated with class 1 *BRAF* mutation in the Western population.

Recognizing the co-occurrence of *BRAF* V600E with other gene mutations in CRC patients is important because that may affect treatment outcomes. Several studies have shown that potential biomarkers including high *BRAF* allele scores (≥2%) (17), *RNF43* mutation (18), consensus molecular subtypes (CMS) (19), and *POLD1*/*POLE* mutation (32) might bring clinical benefits from different treatment modalities. In our study, we found co-mutation features of *BRAF* mutations with other genes such as *KRAS*, *APC*, *PTEN*, and *TP53*. Therefore, identifying and evaluating the co-mutation status of *BRAF* and other genes in CRC patients will help develop personalized treatment strategies. For example, patients with *BRAF* and *KRAS* co-mutations have shown to have a poorer prognosis compared to patients with *BRAF* or *KRAS* mutations alone (33). In addition, co-mutations of *BRAF* have been associated with resistance to chemotherapy and poor survival outcomes and may benefit from immunotherapy (34,35). The limitation

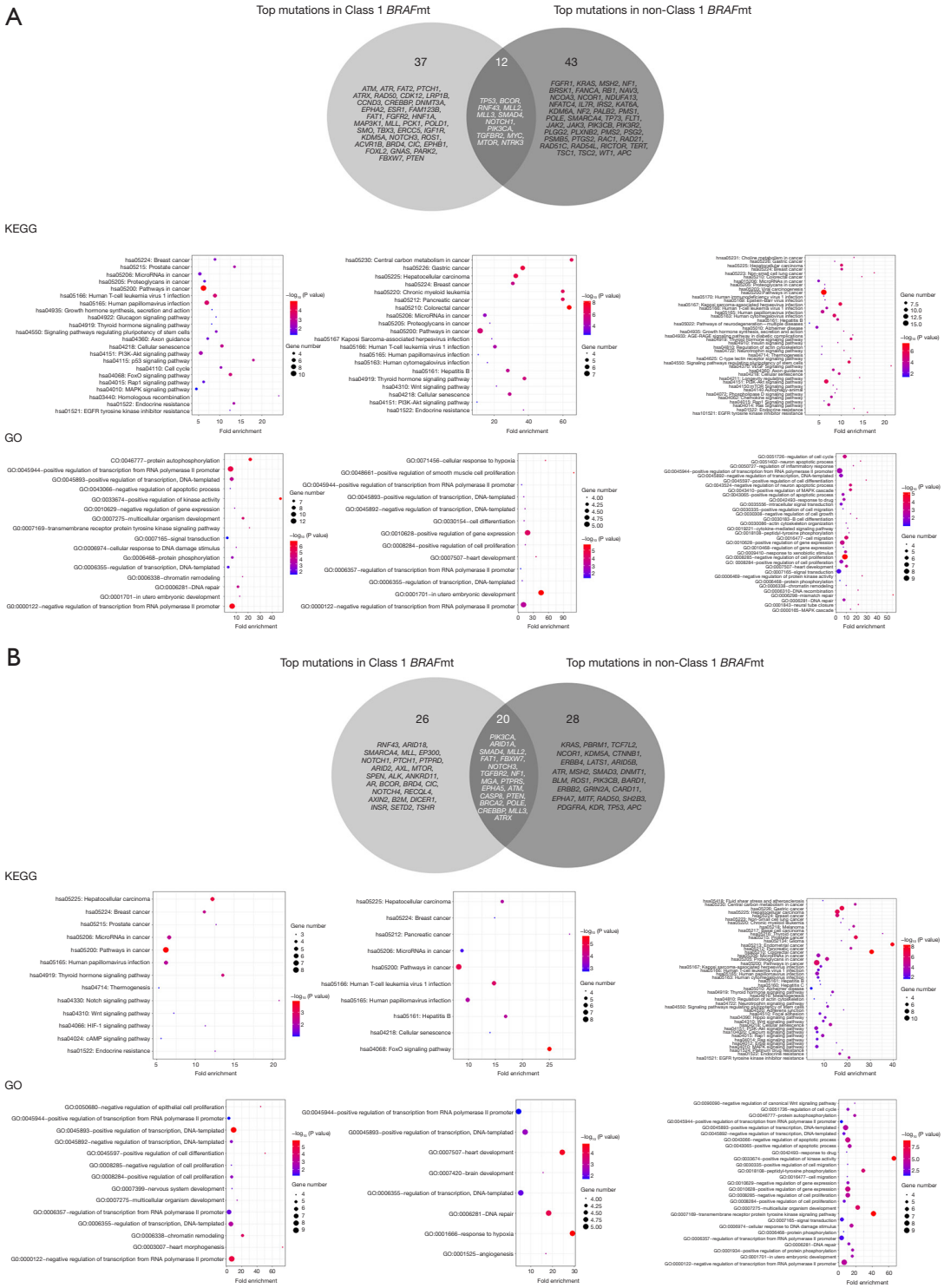

Figure 4 Unique and shared mutation analyses between class 1 and non-class 1 *BRAF* mutations to predict carcinogenicity. The Venn diagram shows the unique and shared mutations of class 1 and non-class 1 *BRAF* mutations in the Chinese cohort (A) and the Western cohort (B). GO and KEGG functional enrichment analyses of differentially unique and shared mutations. The left side shows the class 1 *BRAF*-mutated unique mutations; the middle shows the shared mutations between class 1 and non-class 1 cohort; the right side shows the non-class 1 *BRAF*-mutated unique mutations. mt, mutation; GO, Gene Ontology; KEGG, Kyoto Encyclopedia of Genes and Genomes.

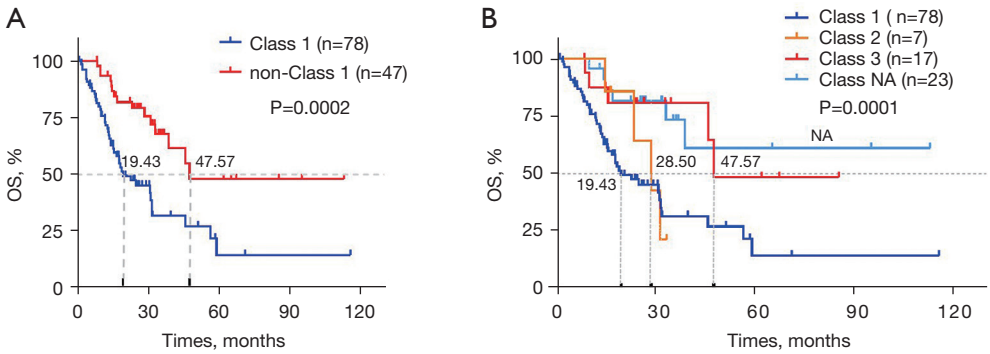

Figure 5 KM analysis of the OS in the 125 *BRAF*-mutated CRC patients. (A) KM analysis of OS between class 1 *BRAF*-mutated and non-class 1 *BRAF*-mutated CRC patients. (B) KM analysis of OS between class 1/2/3/NA *BRAF*-mutated CRC patients. OS, overall survival; NA, not available; KM, Kaplan-Meier; CRC, colorectal cancer.

of this study is that it is retrospective and it is not possible to obtain neat treatment and PFS/OS data. Therefore, this study only conducted prognostic correlation analysis for *BRAF* mutation types. Furtherly, prospective clinical trials are needed to explore therapeutic benefits.

Based on the results of this study, we observed a significant association between *BRAF* mutations and TMB-H and MSI-H. However, TMB-H may be associated with MSI-H rates in patients with BRAF-mutated tumors, which is consistent with published literature (36) showing that a majority of MSI-H samples are also TMB-H (83%), and 97% had TMB ≥10 mutations/Mb. These findings suggest that immunotherapy may be an effective treatment option for CRC patients with *BRAF* V600E mutations. Now we all know targeted therapy may also be a viable treatment option for CRC patients with *BRAF* V600E. Several targeted therapies, such as vemurafenib and dabrafenib, have been approved by the Food and Drug Administration (FDA) for the treatment of *BRAF* V600E melanoma and second-line for mCRC. Recently, in addition to targeted therapy, several clinical trials have shown that immune checkpoint inhibitors, such as pembrolizumab and nivolumab, are effective in treating *BRAF* V600E CRC (37,38). One of the most promising agents is pembrolizumab, which has been approved by the FDA for the treatment of advanced CRC with specific genetic mutations, including *BRAF* V600E (39). Therefore, combining immunotherapy with targeted therapy may be a better choice for treating CRC patients with *BRAF* V600E in China. However, further studies are needed to validate these findings and to determine the optimal treatment strategy for CRC patients with *BRAF* V600E.

Conclusions

In conclusion, our study showed that immunotherapy and targeted therapy may be effective treatment options for CRC patients with *BRAF* V600E, particularly when combined with targeted therapies. However, the co-occurrence of *BRAF* with other gene mutations in CRC patients may affect treatment outcomes, and personalized treatment strategies are needed. Further studies are warranted to validate these findings and to identify optimal treatment regimens for CRC patients with *BRAF* V600E.

Acknowledgments

A part of the manuscript has been presented in ASCO 2023 annual meeting (doi: 10.1200/JCO.2023.41.16_suppl.e15634). A main conclusion of the manuscript has not been published previously. We agree to transfer copyright and assign all rights to the manuscript (and any revisions or versions of it) solely to the journal, to print, publish, distribute, and sell the article in all languages and media internationally.

Funding: None.

Footnote

Reporting Checklist: The authors have completed the STROBE reporting checklist. Available at https://cco.amegroups.com/article/view/10.21037/cco-23-117/rc

Data Sharing Statement: Available at https://cco.amegroups.com/article/view/10.21037/cco-23-117/dss

Peer Review File: Available at https://cco.amegroups.com/article/view/10.21037/cco-23-117/prf

Conflicts of Interest: All authors have completed the ICMJE uniform disclosure form (available at https://cco.amegroups.com/article/view/10.21037/cco-23-117/coif). Z.L. is an employee of Geneplus-Beijing (Beijing, China). The other authors have no conflicts of interest to declare.

Ethical Statement: The authors are accountable for all aspects of the work in ensuring that questions related to the accuracy or integrity of any part of the work are appropriately investigated and resolved. The study was conducted in accordance with the Declaration of Helsinki (as revised in 2013). The study was approved by the Ethics Committee of Beijing Hospital (No. 2023BJYYEC-103-01) and informed consent was taken from all the patients.

References

1. Sung H, Ferlay J, Siegel RL, et al. Global Cancer Statistics 2020: GLOBOCAN Estimates of Incidence and Mortality Worldwide for 36 Cancers in 185 Countries. CA Cancer J Clin 2021;71:209-49.
2. Siegel RL, Miller KD, Fuchs HE, et al. Cancer Statistics, 2021. CA Cancer J Clin 2021;71:7-33. Erratum in: CA Cancer J Clin 2021;71:359.
3. Chen W, Zheng R, Baade PD, et al. Cancer statistics in China, 2015. CA Cancer J Clin 2016;66:115-32.
4. Abushukair HM, Zaitoun SM, Saeed A. Insight on BRAF(V600E) mutated colorectal cancer immune microenvironment. World J Gastrointest Oncol 2022;14:1213-5.
5. Huang Y, Jia W, Zhao G, et al. Analysis of driver gene mutations in colorectal cancer by using next-generation sequencing. Chinese Journal of Geriatrics 2021;12:646-9.
6. Tabernero J, Ros J, Élez E. The Evolving Treatment Landscape in BRAF-V600E-Mutated Metastatic Colorectal Cancer. Am Soc Clin Oncol Educ Book 2022;42:1-10.
7. Guan WL, Qiu MZ, He CY, et al. Clinicopathologic Features and Prognosis of BRAF Mutated Colorectal Cancer Patients. Front Oncol 2020;10:563407.
8. Morkel M, Riemer P, Bläker H, et al. Similar but different: distinct roles for KRAS and BRAF oncogenes in colorectal cancer development and therapy resistance. Oncotarget 2015;6:20785-800.
9. Chen G, McQuade JL, Panka DJ, et al. Clinical, Molecular, and Immune Analysis of Dabrafenib-Trametinib Combination Treatment for BRAF Inhibitor-Refractory Metastatic Melanoma: A Phase 2 Clinical Trial. JAMA Oncol 2016;2:1056-64.
10. Planchard D, Groen HJ, Kim TM, et al. Interim results of a phase II study of the BRAF inhibitor (BRAFi) dabrafenib (D) in combination with the MEK inhibitor trametinib (T) in patients (pts) with BRAF V600E mutated (mut) metastatic non-small cell lung cancer (NSCLC). J Clin Oncol 2015;33:8006.
11. Sosman JA, Kim KB, Schuchter L, et al. Survival in BRAF V600-mutant advanced melanoma treated with vemurafenib. N Engl J Med 2012;366:707-14.
12. Corcoran RB, Atreya CE, Falchook GS, et al. Combined BRAF and MEK Inhibition With Dabrafenib and Trametinib in BRAF V600-Mutant Colorectal Cancer. J Clin Oncol 2015;33:4023-31.
13. Tabernero J, Grothey A, Van Cutsem E, et al. Encorafenib Plus Cetuximab as a New Standard of Care for Previously Treated BRAF V600E-Mutant Metastatic Colorectal Cancer: Updated Survival Results and Subgroup Analyses from the BEACON Study. J Clin Oncol 2021;39:273-84.
14. Kopetz S, Guthrie KA, Morris VK, et al. Randomized Trial of Irinotecan and Cetuximab With or Without Vemurafenib in BRAF-Mutant Metastatic Colorectal Cancer (SWOG S1406). J Clin Oncol 2021;39:285-94.
15. Prahallad A, Sun C, Huang S, et al. Unresponsiveness of colon cancer to BRAF(V600E) inhibition through feedback activation of EGFR. Nature 2012;483:100-3.
16. Corcoran RB, Ebi H, Turke AB, et al. EGFR-mediated re-activation of MAPK signaling contributes to insensitivity of BRAF mutant colorectal cancers to RAF inhibition with vemurafenib. Cancer Discov 2012;2:227-35.
17. Ros J, Matito J, Villacampa G, et al. Plasmatic BRAF-V600E allele fraction as a prognostic factor in metastatic colorectal cancer treated with BRAF combinatorial treatments. Ann Oncol 2023;34:543-52.
18. Elez E, Ros J, Fernández J, et al. RNF43 mutations predict

response to anti-BRAF/EGFR combinatory therapies in BRAF(V600E) metastatic colorectal cancer. Nat Med 2022;28:2162-70.
19. Kopetz S, Murphy D, Pu J, et al. Molecular correlates of clinical benefit in previously treated patients (pts) with BRAF V600E-mutant metastatic colorectal cancer (mCRC) from the BEACON study. J Clin Oncol 2021;39:3513.
20. Yao Z, Yaeger R, Rodrik-Outmezguine VS, et al. Tumours with class 3 BRAF mutants are sensitive to the inhibition of activated RAS. Nature 2017;548:234-8.
21. Dankner M, Rose AAN, Rajkumar S, et al. Classifying BRAF alterations in cancer: new rational therapeutic strategies for actionable mutations. Oncogene 2018;37:3183-99.
22. Yaeger R, Chatila WK, Lipsyc MD, et al. Clinical Sequencing Defines the Genomic Landscape of Metastatic Colorectal Cancer. Cancer Cell 2018;33:125-136.e3.
23. Mondaca S, Walch H, Nandakumar S, et al. Specific Mutations in APC, but Not Alterations in DNA Damage Response, Associate With Outcomes of Patients With Metastatic Colorectal Cancer. Gastroenterology 2020;159:1975-1978.e4.
24. Li H, Durbin R. Fast and accurate short read alignment with Burrows-Wheeler transform. Bioinformatics 2009;25:1754-60.
25. Cibulskis K, Lawrence MS, Carter SL, et al. Sensitive detection of somatic point mutations in impure and heterogeneous cancer samples. Nat Biotechnol 2013;31:213-9.
26. McKenna A, Hanna M, Banks E, et al. The Genome Analysis Toolkit: a MapReduce framework for analyzing next-generation DNA sequencing data. Genome Res 2010;20:1297-303.
27. Robinson JT, Thorvaldsdóttir H, Winckler W, et al. Integrative genomics viewer. Nat Biotechnol 2011;29:24-6.
28. Wang K, Li M, Hakonarson H. ANNOVAR: functional annotation of genetic variants from high-throughput sequencing data. Nucleic Acids Res 2010;38:e164.
29. Peng W, Li B, Li J, et al. Clinical and genomic features of Chinese lung cancer patients with germline mutations. Nat Commun 2022;13:1268.
30. Wang J, Yi Y, Xiao Y, et al. Prevalence of recurrent oncogenic fusion in mismatch repair-deficient colorectal carcinoma with hypermethylated MLH1 and wild-type BRAF and KRAS. Mod Pathol 2019;32:1053-64.
31. Niu B, Ye K, Zhang Q, et al. MSIsensor: microsatellite instability detection using paired tumor-normal sequence data. Bioinformatics 2014;30:1015-6.
32. Garmezy B, Gheeya JS, Thein KZ, et al. Correlation of pathogenic POLE mutations with clinical benefit to immune checkpoint inhibitor therapy. J Clin Oncol 2020;38:3008.
33. Won DD, Lee JI, Lee IK, et al. The prognostic significance of KRAS and BRAF mutation status in Korean colorectal cancer patients. BMC Cancer 2017;17:403.
34. Taieb J, Lapeyre-Prost A, Laurent Puig P, et al. Exploring the best treatment options for BRAF-mutant metastatic colon cancer. Br J Cancer 2019;121:434-42.
35. Park R, Lopes L, Lee S, et al. The prognostic and predictive impact of BRAF mutations in deficient mismatch repair/microsatellite instability-high colorectal cancer: systematic review/meta-analysis. Future Oncol 2021;17:4221-31.
36. Chalmers ZR, Connelly CF, Fabrizio D, et al. Analysis of 100,000 human cancer genomes reveals the landscape of tumor mutational burden. Genome Med 2017;9:34.
37. Ros J, Saoudi N, Baraibar I, et al. Encorafenib plus cetuximab for the treatment of BRAF-V600E-mutated metastatic colorectal cancer. Therap Adv Gastroenterol 2022;15:17562848221110644.
38. Morris VK, Parseghian CM, Escano M, et al. Phase I/II trial of encorafenib, cetuximab, and nivolumab in patients with microsatellite stable, BRAFV600E metastatic colorectal cancer. J Clin Oncol 2022;40:12.
39. Casak SJ, Marcus L, Fashoyin-Aje L, et al. FDA Approval Summary: Pembrolizumab for the First-line Treatment of Patients with MSI-H/dMMR Advanced Unresectable or Metastatic Colorectal Carcinoma. Clin Cancer Res 2021;27:4680-4.

Cite this article as: Huang Y, JiaW, Zhao G, Zhao Y, Zhang S, Li Z, Wu G. Clinical features and mutation analysis of class 1/2/3 *BRAF* mutation colorectal cancer. Chin Clin Oncol 2024;13(1):3. doi: 10.21037/cco-23-117

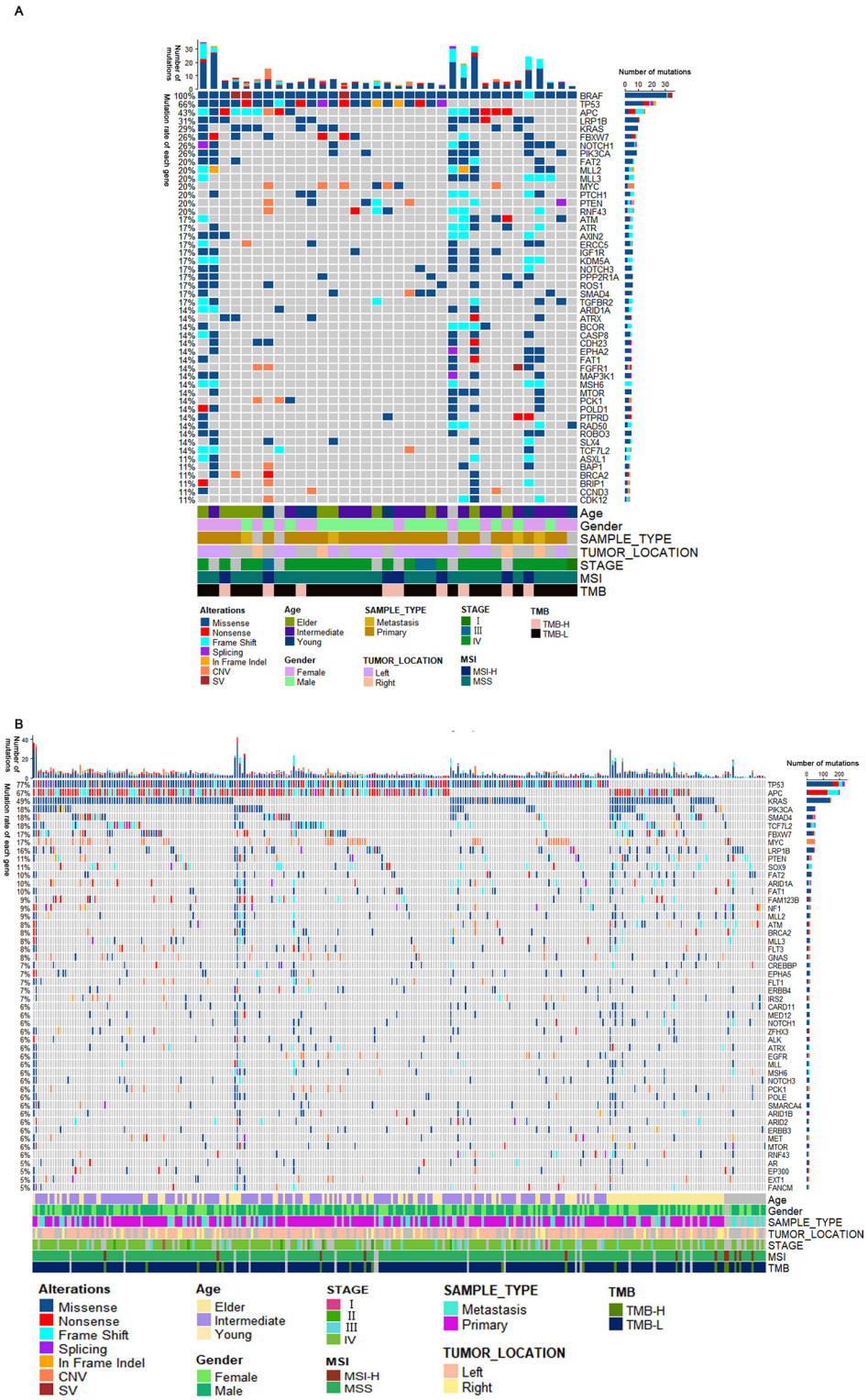

Figure S1 Top 50 mutation spectrum of 339 patients in Chinese cohort (A, *BRAF*-mutated; B, *BRAF* wild-type). Each column represents a patient and each row represents a gene. Table on the left represents the mutation rate of each gene. Top plot represents the overall number of mutations a patient carried. Different colors denote different types of mutation. CNV, copy number variation; MSI, microsatellite instability; MSI-H, high MSI; MSS, microsatellite stability; TMB, tumor mutational burden; SV, structural variation.

https://dx.doi.org/10.21037/cco-23-117

Figure S2 Unique and shared mutation analyses between *BRAF* mutations and *BRAF* wild-type to predict carcinogenicity. The Venn diagram shows the unique and shared mutations of *BRAF* mutations and *BRAF* wild-type in the Chinese cohort. GO and KEGG functional enrichment analyses of differentially unique and shared mutations. The left side shows the *BRAF*-mutated unique mutations; the middle shows the shared mutations between *BRAF* mutations and *BRAF* wild-type; the right side shows the *BRAF* wild-type unique mutations. mt, mutation; GO, Gene Ontology; KEGG, Kyoto Encyclopedia of Genes and Genomes.

https://dx.doi.org/10.21037/cco-23-117